Dynamic Frequency Response From Controlled Domestic Heat Pumps

Mazin T. Muhssin, *Member, IEEE*, Liana M. Cipcigan, *Member, IEEE*, Nick Jenkins, *Fellow, IEEE*, Shane Slater, Meng Cheng, and Zeyad A. Obaid, *Member, IEEE*

***Abstract*—The capability of domestic heat pumps to provide dynamic frequency response to an electric power system was investigated. A thermal model was developed to represent a population of domestic heat pumps. A decentralized dynamic control algorithm was developed, enabling the heat pumps to alter their power consumption in response to a system frequency. The control algorithm ensures a dynamic relationship between the temperature of building and grid frequency. The availability of heat pumps to provide low-frequency response was obtained based on data supplied by Element Energy. Case studies were carried out by connecting a representative model of the aggregated heat pumps to the regional Great Britain (GB) transmission system model, which was developed by National Grid. It was shown that the dynamically controlled heat pumps distributed over GB zones have a significant impact on the GB system frequency and reduce the dependency on frequency services that are currently supplied by expensive frequency-sensitive generators. The rate of change of frequency was also reduced when there is a reduction in system inertia.**

***Index Terms*—Demand side response, dynamic frequency control, electric power system, domestic heat pumps, temperature control, smart grid.**

I. Introduction

WITHIN Great Britain's (GB) power system, the standard operating frequency is 50 Hz, with the upper/lower operating limit being ±1% Hz of nominal system frequency i.e., ±0.5 Hz [1]. National Grid, as the System Operator in the UK, procures frequency response services from the generators through the Mandatory Frequency Response (MFR) service [2]. All large generators covered by the GB Grid Code must be capable of providing three types of frequency service. The primary low-frequency response service provides an additional active power (or decrease in power of demand) within 10 seconds, continuing for a further 20 seconds. The secondary response service provides low-frequency response within 30 seconds, after an incident, and lasts for another 30 minutes. For a loss in power demand incident, the high-frequency response service reduces the active generation power within 10 seconds and can be continued until the frequency is restored to 50 Hz. Maintaining an instantaneous balance between generation and demand is becoming increasingly difficult, due to the increase in the use of renewable energy resources [3]. Integration of wind turbine generators that are mechanically decoupled from the grid, reduces the inertia of the power system and causes the rate of change of frequency (RoCoF) to become more rapid [4]. Thus, a faster frequency response is required to overcome such challenges. The cost of additional frequency response under existing arrangements is expected to increase to £250 million per annum, by 2020, if no alternative technologies will be developed [4].

In its 2015 "System Operability Framework" report, National Grid, discusses new innovative control mechanisms, on the demand side, in order to provide rapid frequency response services and reduce the CO_2 emissions at a reasonable cost [5]. Demand Side Response (DSR) is one of these mechanisms that can be used to increase or decrease the power demand of some devices, in order to regulate the system frequency when either: unpredicted fluctuations of power occur or during outages of one or several generation units [6]. In the present GB power system, some industrial loads participate in frequency control service through the Frequency Control by Demand Side Management (FCDM) service. Such controlled electricity demand is interrupted when system frequency transgresses a large low-frequency relay setting (typically 49.7 Hz) and usually requires manual reconnection [7]. There are a wide variety of ways in which demand can provide frequency responses. Against the background of previous research, two main load frequency control forms are recognised; centralised and localised control.

In [8]–[10], a centralised control algorithm was presented to regulate the system frequency by controlling the aggregation of small loads such as electric water heating. The power system operator operates the central controller which monitors the condition of all loads and switches them ON or OFF in response to an external signal. Thermal loads are time-flexible loads that can provide frequency regulation without harming customer comfort. For instance, [11] examined a centralised thermostatically controlled load algorithm of a population of heating appliances, such as heating ventilation and air-conditioning (HVAC) and water heater. The central controller is equipped with a temperature forecaster to estimate the temperature of the building

Manuscript received April 28, 2017; revised September 21, 2017 and November 21, 2017; accepted December 23, 2017. Date of publication January 18, 2018; date of current version August 22, 2018. This work was supported in part by Cardiff University, U.K., in part by National Grid, Warwick, U.K., and in part by the HCED, Iraq. Paper no. TPWRS-00629-2017. *(Corresponding author: Mazin T. Muhssin.)*

M. T. Muhssin, L. M. Cipcigan, N. Jenkins, M. Cheng, Z. A. Obaid are with the Institute of Energy, School of Engineering, Cardiff University, Cardiff CF10 3AT, U.K. (e-mail: mazinthany2004@gmail.com; CipciganLM@cardiff.ac.uk; JenkinsN6@cardiff.ac.uk; ChengM2@cardiff.ac.uk; AlObaidiZA@cardiff.ac.uk).

S. Slater is with Element Energy, Cambridge CB5 8AQ, U.K. (e-mail: shane.slater@element-energy.co.uk).

Color versions of one or more of the figures in this paper are available online at http://ieeexplore.ieee.org.

Digital Object Identifier 10.1109/TPWRS.2017.2789205

and switch the HVAC in response to an external signal only at specific temperature levels. However, the centralised control approach requires a complex and costly two-way communication between the load and an upper layer, such as aggregators, the distribution and transmission system operators. Therefore, a localised load control was developed to provide a local frequency control, avoiding the complexity and the time delay accompanied by two-way communication with the network operator. The basic operation of the localised load control can be summarised as turning loads ON or OFF when frequency goes above or below pre-defined threshold values [12], [13].

Several studies have addressed the dynamic frequency control from thermal loads such as industrial bitumen tanks in [14], and domestic refrigerators in [13] and [15]. The potential of different types of domestic loads to provide dynamic demand service was presented in [16]. In these papers, the temperature set-points of thermal loads were controlled to vary dynamically with grid frequency.

II. Scope

Heat pumps have become increasingly common in the UK [5]. By 2030, domestic heat pumps could provide an average low-frequency response of 2GW as it was presented in the winter medium uptake scenario of the Element Energy [17].

This paper examines the potential of the aggregation of domestic heat pumps to provide a dynamic frequency response to the GB power system. The heat pumps' control is hereafter referred to as Dynamic Frequency Control (DFC). There are still challenges to the use of DFC in large power systems as shown in papers [13] and [14]. Each type of appliance requires a different thermal model, a suitable model to represent a population of appliances connected to the system, and a different load control characteristic. This paper identifies a suitable model that represents the entire population of heat pumps connected to the GB power system. A new DFC method that controls the heat pumps' power consumption in response to the system frequency is developed without undermining the inherent operation of heat pumps. The proposed DFC algorithm was validated through the integration of the whole model, into the GB transmission reduced system model. This study addresses the following questions.

- Is there a suitable number of heat pump aggregated models that can represent the entire population of heat pumps, connected to the GB power system?
- How to improve the dynamic operation of the load's triggering frequencies (F_{ON}) and (F_{OFF})?
- Does DFC interfere with the normal operation of heat pumps' temperature control?
- What impact will the population of DFC-based heat pumps have on grid frequency?
- Do DFC-based heat pumps reduce the dependency on frequency services that are obtained by expensive peaking generators?
- Does regional DFC affect the system frequency?
- What impact might the DFC have on the rate of change of frequency (RoCoF), when there is a reduction in system inertia?

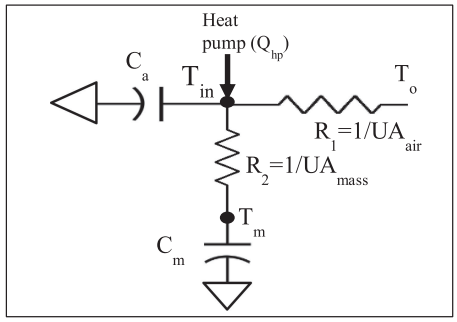

Fig. 1. Equivalent thermal model of a domestic building.

III. Modelling and Simulating of Heat Pumps

A. Modelling of a Population of Heat Pumps

An equivalent thermal parameter (ETP) model was used to represent domestic buildings [18] and [29]. The equivalent electric circuit is shown in Fig. 1. The heat flow into the building is provided through a thermostatically controlled heat pump unit coupled to the ETP model.

C_a = building indoor air heat capacity (J/°C).
C_m = building mass heat capacity (J/°C).
Q_{hp} = heat rate of heat pump unit (W).
UA_{air} = heat loss coefficient (air to the ambient) (W/°C).
UA_{mass} = heat loss coefficient (between air and mass) (W/°C).
R_1 $= 1/UA_{air}$.
R_2 $= 1/UA_{mass}$.
T_{in} = indoor air temperature (°C).
T_m = building mass temperature (°C).
T_o = ambient temperature (°C).

The differential equations description of the thermal model are shown in (1) and (2),

$$C_a \frac{dT_{in}}{dt} = -\frac{1}{R_1}(T_{in} - T_o) - \frac{1}{R_2}(T_{in} - T_m) + Q_{hp} \quad (1)$$

$$C_m \frac{dT_m}{dt} = \frac{1}{R_2}(T_{in} - T_m) \quad (2)$$

Typically, the building mass thermal storage C_m is large and hence, the temperature variation of the building mass dT_m/dt is small. For this reason, it is assumed that $T_{in} = T_m$ according to (2). By considering the equivalent heat capacity $C = C_a + C_m$, the equivalent model is reduced to (3).

$$\frac{dT_{in}}{dt} + \frac{1}{R_1 C} T_{in} = \frac{1}{C}\left(\frac{1}{R_1} T_o + Q_{hp}\right) \quad (3)$$

The differential equation in (3) has two exponential forms depending on the state of the heat pump s_c. As shown in Fig. 2, when the heat pump is switched ON $(s_c = 1)$, the building temperature T_{in} starts from the low temperature set-point $T_{\min}$ at $t = 0$ min and increases until reaching the upper temperature set-point $T_{\max}$ at $t_{on} = 30$ min. When the heat pump is turned OFF $(s_c = 0)$, T_{in} starts from $T_{\max}$ at $t_{off} = 30$ min and decreases until reaching $T_{\min}$ at $t_{off} = 60$ min. Therefore, the time constants τ_{on} and τ_{off} of the heat pump's ON and OFF cycles can be defined as in (4) and (5).

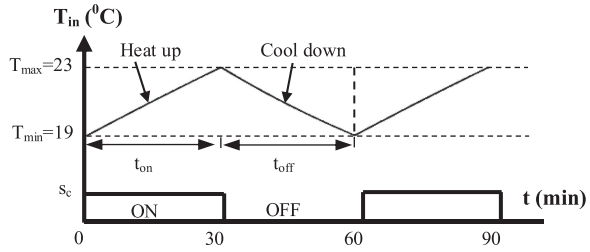

Fig. 2. Temperature control of one heat pump unit.

TABLE I
MODEL PARAMETERS

C (J/°C)	R_1 (°C/W)	T_0 (°C)	T_{max} (°C)	T_{min} (°C)
3600	0.121	8	23	19

The mean values of R_1 and C are shown in Table I. These parameters were calibrated based on temperature measurement of a typical domestic building [19].

$$\tau_{on} = \frac{t_{on}}{R_1 C} 1/\ln\left(\frac{T_{\min} - T_0 - Q_{hp}R_1}{T_{\max} - T_0 - Q_{hp}R_1}\right) \quad (4)$$

$$\tau_{off} = \frac{t_{off}}{R_1 C} 1/\ln\left(\frac{T_{\min} - T_0}{T_{\max} - T_0}\right) \quad (5)$$

The temperature set-points $T_{\min}$ and $T_{\max}$ were set to 19 °C and 23 °C to represent a dwelling insulated to typical UK levels [20]. With such temperature levels, the heat pump's cycle time is almost one hour. According to the Element Energy study [17], it was assumed that each heat pump has a power consumption of 3 kW. This power was chosen to be the lower value of the typical range for domestic heat pumps in the UK.

By solving the differential equation in (3) and defining the time constants in (4) and (5), two exponential forms for T_{in} based on heat pump state s_c were found, as shown in (6) and (7).

$$T_{in} = 58.34 - 39.34 \times e^{-0.0036t} \quad s_c = 1 : 0 \le t < t_{on} \quad (6)$$

$$T_{in} = 10 - 12.99 \times e^{-0.0122t} \quad s_c = 0 : \ t_{on} \le t < t_{off} \quad (7)$$

Equations (6) and (7) were used to simulate a single domestic building equipped with a heat pump unit. However, a single ETP model with different thermal parameters can be used to represent a large number of domestic buildings [18]. The thermal parameters (R_1 and C) that are required to compute the load vary between buildings. The expected thermal parameters values for different types of UK houses were modelled in [21], using parameter estimation techniques. In this paper, the population of domestic buildings was modelled by giving ranges to the thermal parameters, where every building was assigned randomly with different values of R_1 in the range $(0.005 - 1.177)$ °C/W and C in the range (3,263–15,000) J/°C.

To reflect the diversity among a population of heat pumps, a different initial temperature was chosen for each building by randomising the starting time in (6) and (7) using a uniform distribution.

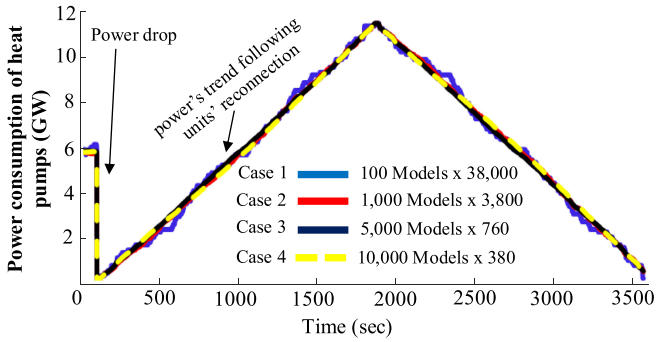

Fig. 3. Total Power Consumption of 3.8 million heat pumps obtained from the thermodynamic model.

B. Identification of Suitable Number of Heat Pump Models

According to the 2030 medium uptake scenario of Element Energy [17], there are expected to be 3.8 million heat pumps in UK dwellings by 2030.

[22] shows that the demand coincidence factor remains constant when the number of consumers is more than 5,000. This means that the ratio between the total number of appliances (greater than 5,000) and the number of appliances that would operate (consume electricity) is approximately constant. However, the coincidence factor might be slightly different from one type of load to another. Therefore, it is infeasible to have 3.8 million independent heat pump models. Instead, aggregated models were developed. Each heat pump has different initial ON/OFF state and each building has different initial T_{in}. As shown in Fig. 3, following a drop of power at time 100 sec (all heat pumps were switched OFF at this time), the power consumption behaviour of four case studies of different numbers of heat pumps in each aggregation were compared. Fig. 3 shows the power consumption of 100, 1,000, 5,000 and 10,000 aggregated heat pump models. The response of the aggregated models with 5,000 and 10,000 heat pumps were more gradual and had a similar power consumption behaviour. The aggregated model, with 5,000 heat pumps multiplied by scaling number 760, was chosen as the best model to represent the entire population of heat pumps based on accuracy and simulation time.

IV. CONTROL OF HEAT PUMPS

A. Temperature Control of Heat Pumps

A diagram of the Temperature Controller of a heat pump unit is shown in Fig. 4. The temperature control is used to maintain the building temperature within set-points $T_{\min}$ and $T_{\max}$. The temperature control measures the building temperature T_{in} and generates temperature state signal S_T. If T_{in} reaches $T_{\max}$, the temperature controller sets S_T to '0' and heat pump is turned OFF. If T_{in} reaches $T_{\min}$, the temperature controller sets S_T to '1' and heat pump is turned ON.

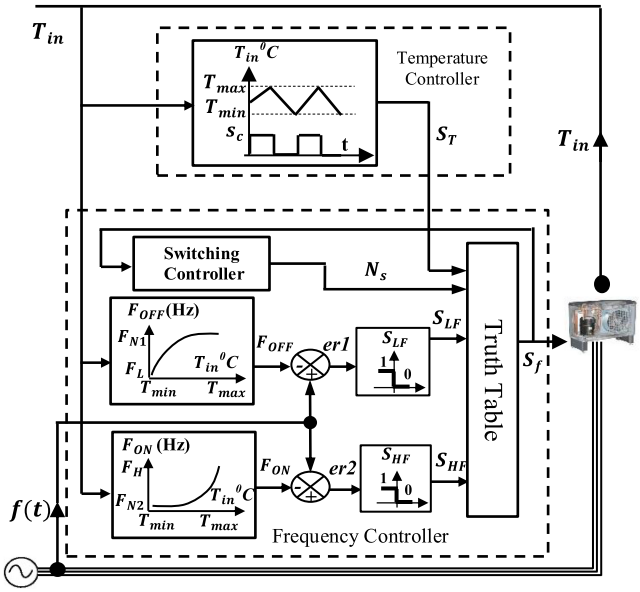

Fig. 4. Diagram of DFC scheme of a heat pump.

TABLE II
LOGIC OPERATION TRUTH TABLE

Row	S_T	S_{LF}	S_{HF}	$if\ N_S = 0$
1	0	0	0	$S_f = 0$
2	1	0	0	$S_f = 0$
3	0	1	1	$S_f = 1$
4	1	1	1	$S_f = 1$
5	0	0	1	$S_f = S_T$
6	1	0	1	$S_f = S_T$

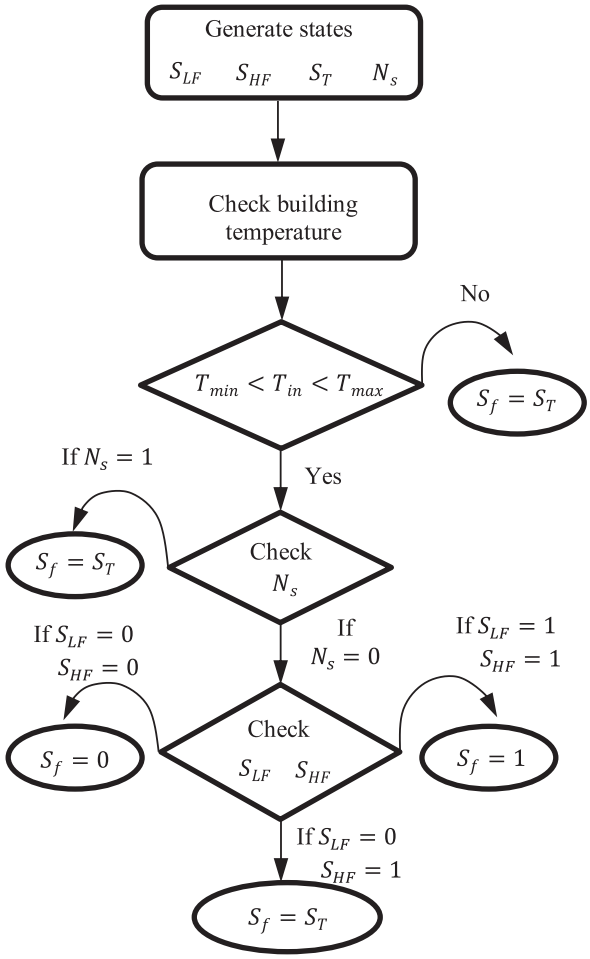

Fig. 5. State transition diagram.

B. Integrated Frequency Control of Heat Pumps

The Frequency Controller was added to the temperature control in Fig. 4. The frequency control is responsible for generating the lower and higher frequency state signals S_{LF} and S_{HF}, by continuously comparing the grid frequency $f(t)$ with the trigger frequencies F_{ON} and F_{OFF}. National Grid assumes a frequency dead-band of ±0.1 Hz, in which no frequency response is needed from an electric load [1]. Therefore, in this study, F_{ON} has a range of 50.1-50.5 Hz and F_{OFF} has a range of 49.5-49.9 Hz. The final switching signal S_f is determined at each sampling time $\Delta t = 0.2$ sec from the state signals S_{LF}, S_{HF}, S_T as shown in Table II. When the system frequency drops lower than F_{OFF}, the S_{LF} and S_{HF} are both switched to '0' and the heat pump is switched OFF $(S_f = 0)$ as presented in rows 1-2.

Similarly, if $f(t)$ rises higher than F_{ON}, the two state signals S_{LF} and S_{HF} turn into '1', and the heat pump is switched ON $(S_f = 1)$ as shown in rows 3-4.

Rows 5-6 are the cases in which there is no frequency event $(F_{OFF} < f(t) < F_{ON})$. The heat pump follows the temperature control signal S_T because $S_{LF} = 0$ and $S_{HF} = 1$.

[23] indicates that the maximum number of switching events should not exceed 3 every half hour, otherwise the heat pump's life time might be degraded. Therefore, a Switching Controller was added to the control system in Fig. 4 to control the maximum number of switching events. The final switching signal S_f is an input to a Switching Controller as shown in Fig. 4. The Switching Controller is responsible for generating a switching state signal N_s to limit the maximum number of heat pump switching events to three every 30 minutes. As shown in Fig. 5, if $N_s = 0$, S_f is determined by the frequency state signals S_{LF}, S_{HF}. If $N_s = 1$, this indicates that the number of switching events has exceeded three within 30 minutes and therefore, the heat pump reverts to temperature control and follows S_T.

The temperature T_{in} is another input to the frequency controller. As seen in Fig. 5, if T_{in} is outside the set-points $T_{\min}$ or $T_{\max}$, the temperature state signal S_T is prioritized and the frequency controller will not be triggered.

When the heat pump is turned OFF the power demand is reduced quickly (typically in milliseconds); however, if the heat pump is turned ON, the increase of its power could take tens of seconds depending on the type of heat pump [17, p. 53]. Also, the response of the heat pump depends significantly on the liquid refrigerant cycle inside it. That is, if the heat pump is turned OFF and then turned ON in a very short period of time, the compressor might be damaged because the refrigerant pressure has not been equalized. In this study, a minimum ON/OFF time

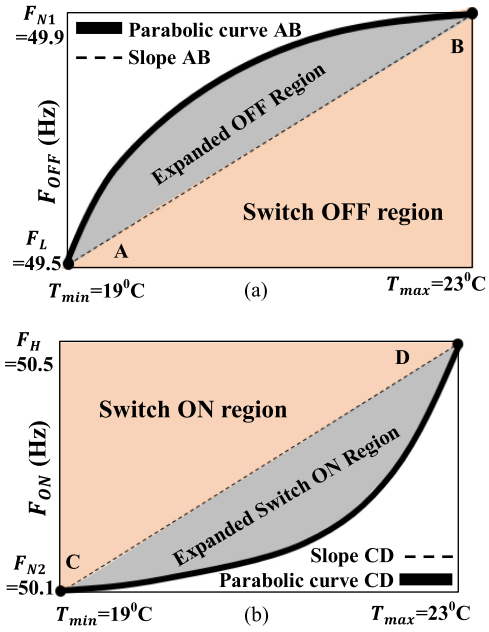

Fig. 6. Dynamic trigger frequencies (a) F_{OFF} varies with T_{in} (b) F_{ON} varies with T_{in}.

delay of at least 1min was applied to avoid frequent switching actions which may damage the heat pump's compressor.

C. Dynamic Trigger Frequencies (F_{OFF} and F_{ON})

It is often assumed that F_{OFF} and F_{ON} are linearly proportional to indoor temperature as shown in Fig. 6 (dashed slope) [13] and [15]. For a frequency drop, heat pumps are switched OFF in descending order starting from the warmest building. For a frequency rise, heat pumps are switched ON in ascending order starting from the coldest building.

In this research, the trigger frequencies F_{ON} and F_{OFF} were chosen to vary dynamically with the building temperature T_{in} according to the parabolic curves AB and CD shown in Fig. 6. These are described by (8) and (9). The lower frequency set point F_L (49.5 Hz) and the higher frequency set point F_H (50.5 Hz) are the same in both the linear (slope) and parabolic methods. However, the variations of the trigger frequencies F_{OFF} and F_{ON} with the building temperature were improved when using the parabolic shape. As shown in Fig. 6, the parabolic shape expands the region of the switching action which causes more heat pumps to respond to the frequency event earlier. The F_{N1} (49.9 Hz) and F_{N2} (50.1 Hz) are the normal frequency set points.

The parabolic curve provides smooth response, and the frequency change can be controlled at an early stage following the frequency incident. Cubic and higher order shapes could be also used to provide fast frequency response service, but they are computationally more complex.

$$F_{OFF} = \frac{F_L - F_{N1}}{(T_{\min} - T_{\max})^2}(T_{in} - T_{\max})^2 + F_{N1} : T_{in} \in [T_{\min}, T_{\max}] \quad (8)$$

$$F_{ON} = \frac{F_H - F_{N2}}{(T_{\max} - T_{\min})^2}(T_{in} - T_{\max})^2 + F_{N2} : T_{in} \in [T_{\min}, T_{\max}] \quad (9)$$

For a frequency drop, the parabolic curve AB shown in Fig. 6(a), will assign F_{OFF} closer to F_{N1} than the linear slope AB. This will switch OFF more heat pumps, especially at the earliest stage following the event and the frequency drop will be halted earlier.

Similarly, for a frequency rise, the parabolic curve CD shown in Fig. 6(b), will assign F_{ON} closer to F_{N2} than the linear slope CD. This will switch ON more heat pumps at the earliest stage following the frequency event and the frequency rise will be controlled earlier.

The DFC has been designed to avoid a large load payback that would result from a simultaneous reconnection of substantial load after the frequency event. As the grid frequency recovers, the heat pumps will be reconnected smoothly (not simultaneously), starting from the buildings with the lower temperature. The fact that a population of buildings will have different temperatures means that heat pumps switching events will be smooth, avoiding simultaneous switching. This reduces the load payback of the heat pumps.

V. Simulation and Discussion of the DFC

This section discusses the operation of the DFC. Fig. 7 shows the impact of the Switching Controller on the number of switching events. Fig. 7 shows that the N_s signal is turned to '1' when there are more than three switching events per half hour, and then the heat pump operates normally, only in response to the temperature. The N_s signal is turned to '0' as long as the number of switching events is still within the acceptable limit.

Fig. 8 shows the performance of the dynamic trigger frequencies. In Fig. 8(a), F_{OFF1-P} and F_{OFF2-P} represent the lower trigger frequencies of two heat pumps were varied with T_{in} based on the Parabolic curve AB, and F_{OFF1-S} and F_{OFF2-S} were varied based on the linear Slope AB. Following a frequency drop, Fig. 8(a) shows that with the use of parabolic curve AB, both heat pumps were switched OFF in response to the frequency drop. With the use of slope AB, only one heat pump was switched OFF.

In Fig. 8(b), F_{ON1-P} and F_{ON2-P} show that the higher trigger frequencies of the two heat pumps were varied based on the Parabolic curve CD, and F_{ON1-S} and F_{ON2-S} were varied based on the linear Slope CD. Following a frequency rise, Fig. 8(b) shows that two heat pumps were switched ON in response to the frequency rise when curve CD was used. However, only one heat pump is switched ON when the linear slope CD was used

In a summary, the trigger frequencies were improved using the parabolic shape, so that more heat pumps have the ability to respond to the frequency change at an early stage following the event.

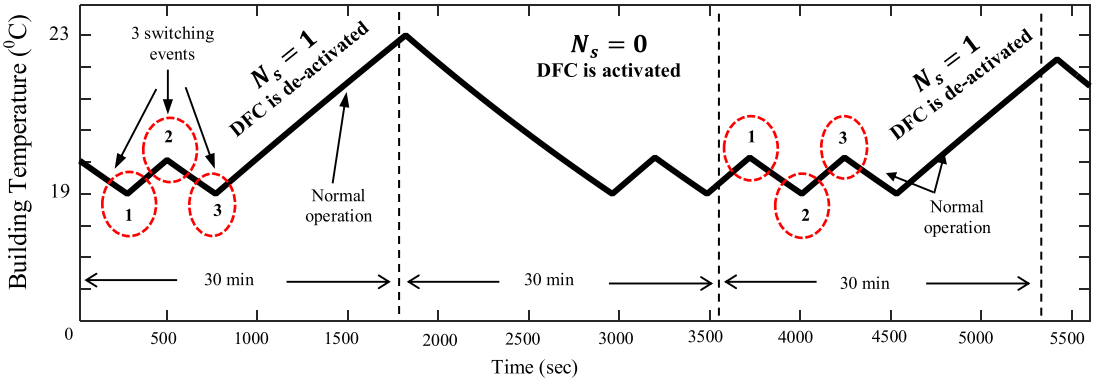

Fig. 7. Effect of the logic control N_s on the operation of heat pump.

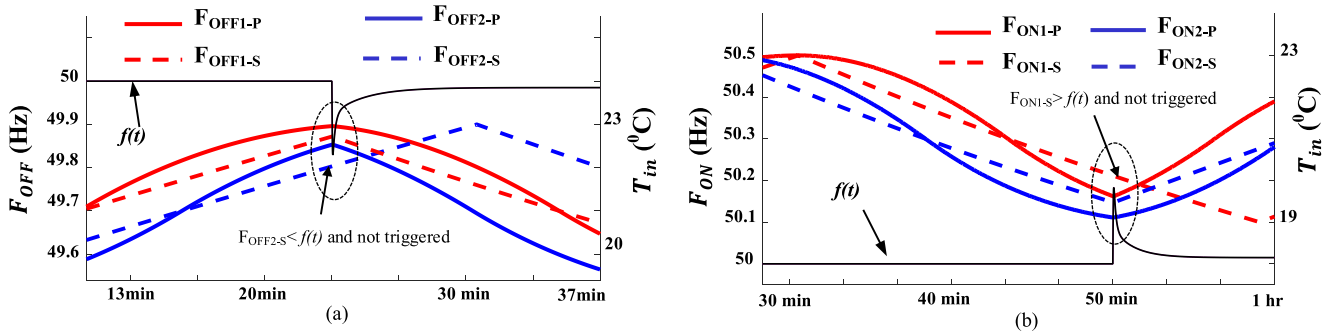

Fig. 8. Comparison of trigger frequencies of two heat pumps. (a) F_{OFF} using Curve AB and Slope AB (b) F_{ON} using Curve CD and Slope CD.

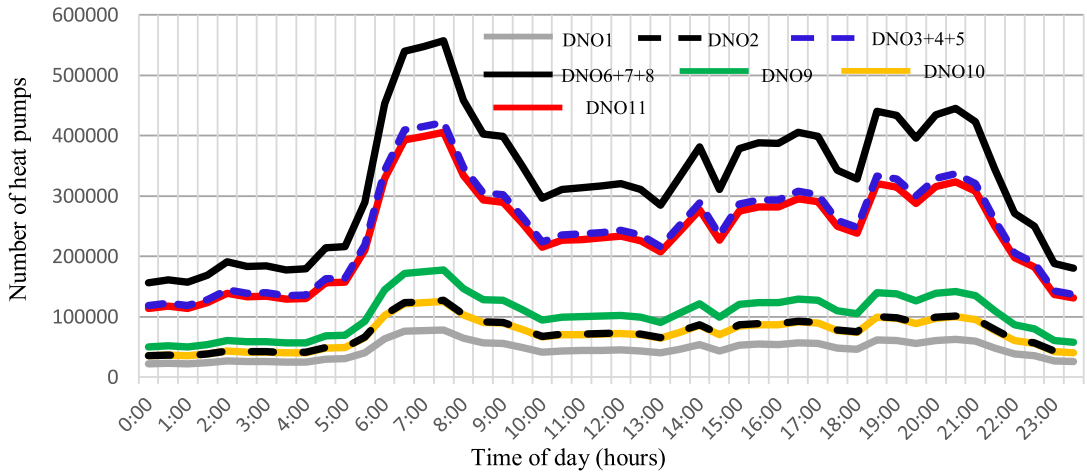

Fig. 9. Diurnal variation in average number of heat pumps (NHP), 2030 winter medium scenario.

VI. Availability of Heat Pumps for Frequency Service

The daily average number of heat pumps in the ON state which are available to be switched OFF in response to a low-frequency response is denoted ONHP. The ONHP was estimated by Element Energy for the 2030 medium uptake scenario of winter months in the Great Britain. In this study, the ONHP data was used as an input to the model to specify the amount of heat pumps that can provide low-frequency response at each time of the day. The average number of heat pumps that are connected to the grid and are in either the ON and OFF states are denoted NHP. The typical ON and OFF cycles of heat pumps were assumed equal. Therefore, the NHP was assumed as twice as the ONHP. The geographical NHPs were calculated based on the number of householders in each area [24], [25]. The daily NHPs of the Great Britain were scaled down to represent the NHPs at each of the eleven distribution network operators (DNOs) in the GB power system. This is described in Fig. 9.

VII. Case Studies on the GB Transmission Model

The heat pump models were integrated into a reduced GB transmission power system, through a collaboration with National Grid. This model is a 36-bus equivalent network

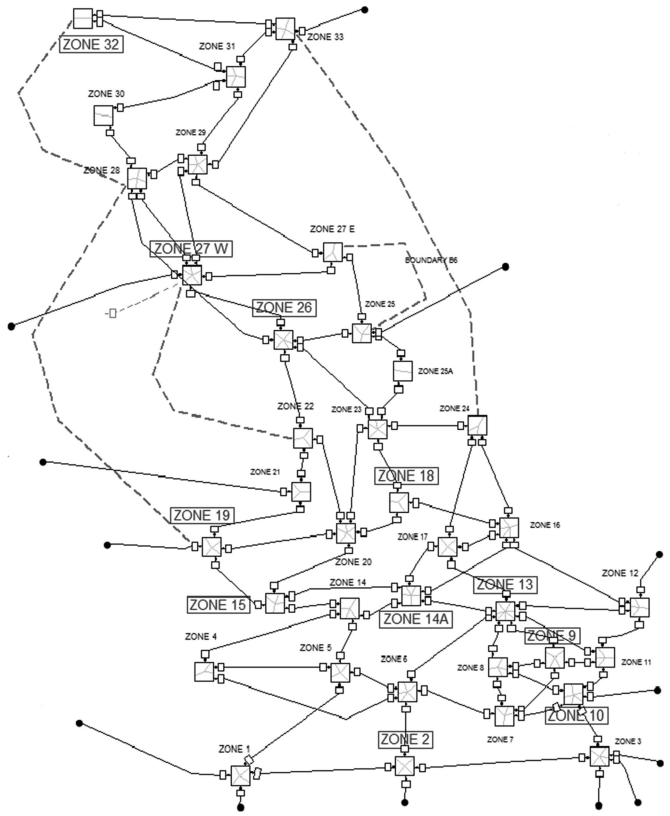

Fig. 10. Reduced GB 36-bus/substation transmission model.

representing the National Electricity Transmission System of Great Britain, which was modelled in DIgSILENT by National Grid, as shown in Fig. 10. It is an electro dynamic model dispatched according to the National Grid Gone Green 2030 Future Energy Scenario. Each geographic zone in the model represents generation, demand and HVDC interconnectors. Generators within each zone are categorised according to fuel types and are represented by synchronous and static generators. The new nuclear stations are concentrated in the south of the GB power network, and the wind farms in Scotland and offshore.

Aggregated heat pump models were assumed to be allocated in the eleven DNO networks of the GB power system. The zones shown in Table III are a close geographical reflection to the GB DNOs [26].

The NHPs in each zone were taken from Fig. 9 at times 11:00-12:00 (the time of frequency event that happened in 2008 [27]) and 17:00–17:30 (representing the winter evening peak time).

A. *Case Study 1*

The case study considered a frequency event with a profile similar to that which occurred in 2008 [27]. That event was caused when two generators (345 MW and 1,237 MW) tripped spontaneously within a short time (11:34 am-11:36 am).

To obtain such a frequency profile on the GB system model, the magnitudes of the loss of generation was changed such that the first loss (690 MW) was applied at time 2 sec in zone 29. The loss of second generator (1,139 MW) was applied after two minutes in zone 12.

TABLE III
NUMBER OF HEAT PUMPS IN EACH ZONE

Zone number	Locations-based DNOs	NHPs at 11:30–12:00	NHPs at 17:00–17:30
Z-32	North Scotland (DNO-1)	44,226	55,795
Z-27W	Central and Southern Scotland (DNO-2)	70,946	89,504
Z-18	North East England (DNO-3)	115,041	145,134
Z-26	North West England (DNO-4)	115,041	145,134
Z-14A	Yorkshire (DNO-5)	115,041	145,134
Z-19	East England (DNO-6)	119,832	151,177
Z-15	London (DNO-7)	119,832	151,177
Z-10	South East England (DNO-8)	119,832	151,177
Z-2	Southern England (DNO-9)	100,776	127,137
Z-9	Merseyside, Cheshire, North Walesand North Shropshire (DNO-10)	71,983	90,812
Z-13	E. Midlands, W. Midlands, S. Wales and S. West England (DNO-11)	316,331	399,077
Total		1,308,881	1,651,258

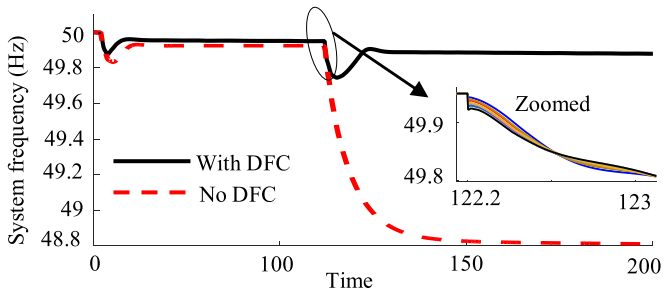

Fig. 11. Variation of frequency at different zones.

The system demand at that time was around 40 GW. The inertia constant of the synchronous generators in the model was set to 5 sec. The NHPs were taken from Fig. 9 as described in Table III at time 11:30–12:00.

Fig. 11 shows the impact of controlled heat pumps on system frequency at different zones. After the first event, the DFC has reduced the frequency drop 0.1 Hz (49.9 Hz from 49.8 Hz). Following the second incident, the DFC has reduced the frequency drop 0.94 Hz (from 48.8 Hz to 49.74 Hz) and maintained the system frequency within the operating limit. The zoomed shape in Fig. 11 shows that the controlled heat pumps distributed over GB zones maintained the frequency deviation in each zone in a nearly similar manner.

Fig. 12 shows the changes in the power consumption drawn by heat pumps at different zones. The heat pumps at different locations provided frequency response in proportion to the frequency deviation. In addition, the locations of heat pumps showed little impact on the frequency response they provided. Fig. 13 shows the change of power output delivered by three aggregated synchronous generators (Nuclear and Gas) (see the right axis) and shows the total power of heat pumps (see the left axis). When the first incident occurred, the power consumption of heat pumps was decreased by 300 MW and after the second incident, it was decreased by a further 600 MW. The power output from synchronous generators was also reduced.

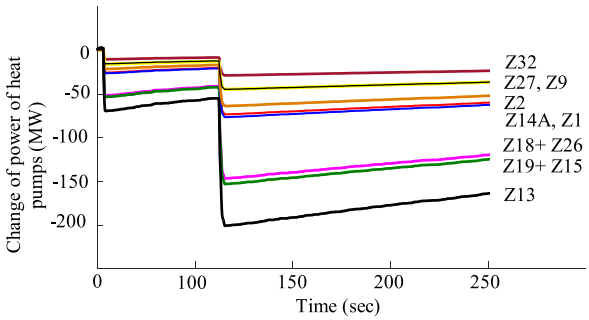

Fig. 12. Power reduction of heat pumps at different zones in the reduced GB transmission system model.

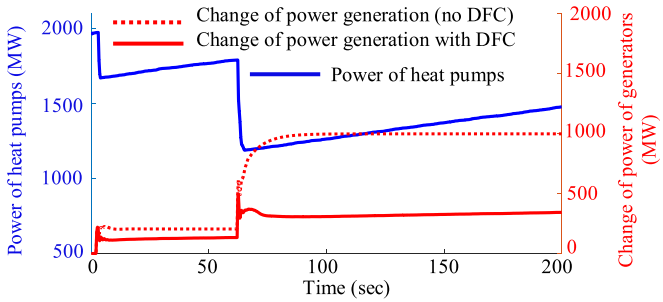

Fig. 13. Change of power output of three aggregated generators at different zones and the total power of heat pumps.

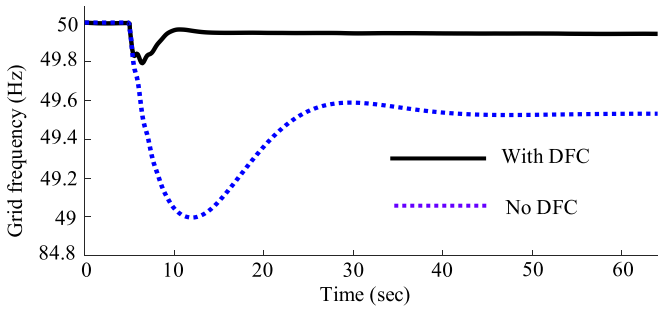

Fig. 14. Variation of frequency (with and without DFC).

B. Case Study 2

The second case study was carried out for low system inertia with much generation assumed to come from converter connected wind turbines [28]. To represent this, the inertia constant of all synchronous generators was changed to 3 sec from 5 sec. The system demand of the model was 39 GW. The NHPs that are available to provide low-frequency response were taken from Fig. 9 at the evening time. This is described in Table III, at time 17:00-17:30.

A 1724 MW synchronous generator located in the centre of the GB network was tripped at time 5 sec. This generator was chosen to be a close reflection to the infrequent infeed loss, i.e., 1800 MW in the GB power system.

Fig. 14 shows that the controlled heat pumps have reduced the frequency drop 0.78 Hz (from 49 Hz to 49.78 Hz) and maintained the system frequency within the standard limit.

Fig. 15 shows the change of power output from eleven aggregated large synchronous generators (>500 MW) (see the right axis) and the power consumption of heat pumps (see the left axis). The power consumption of heat pumps was reduced immediately after the frequency drop exceeded the dead-band limit (49.9 Hz). Also, the dependency on the power output from the large generators was reduced.

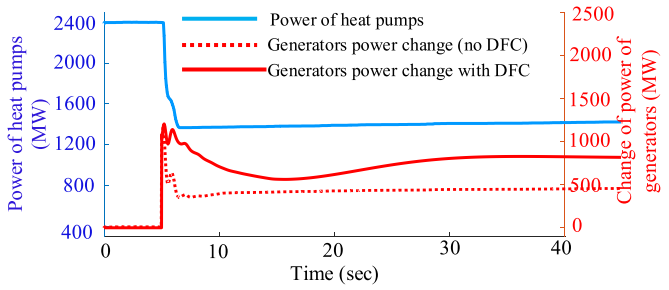

Fig. 15. Change of aggregated power output of large generators (<500 MW) at different zones and the total power of heat pumps.

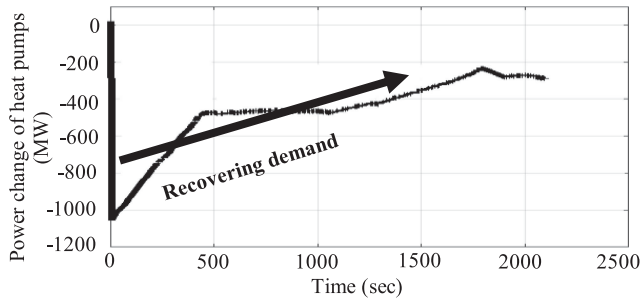

Fig. 16. Total demand of heat pumps during 30 min following the event.

Fig. 16 shows the total change of demand for heat pumps during the half an hour following the event. As can be seen, the DFC effectively reduced 1000 MW from heat pump demand. The heat pump demand recovered within the 30 min following the event. This allowed the system frequency to be restored using stand-by generation (responding after 30 min) instead of using the power from costly spinning reserve responding in real time.

Furthermore, the DFC has caused a little payback after the frequency recovery because the heat pumps have been reconnected gradually, causing a gradual increase of the power consumption.

C. Case Study 3

A case study was carried out to compare the impact of a population of heat pumps using DFC, with parabolic and slope control techniques. The frequency deviation and RoCoF that would result from a large imbalance contingencies ranging from 1.8 GW to 4 GW were investigated, i.e., the size and speed of the power change were very different. National Grid aims to control the threshold level of RoCoF at an early stage following the incident, i.e.,(≤500 msec) [28].

The system inertia was set to 3 sec and system demand to 39 GW. The NHPs were considered as in Table III, at time 17:00–17:30.

Fig. 17 shows that the DFC using parabolic technique halted the system RoCoF faster than the slope technique during the first 500 msec following the incident.

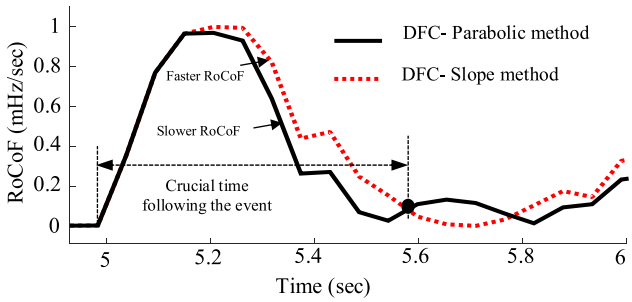

Fig. 17. Rate of Change of grid frequency (RoCoF) (loss of 1.724 GW).

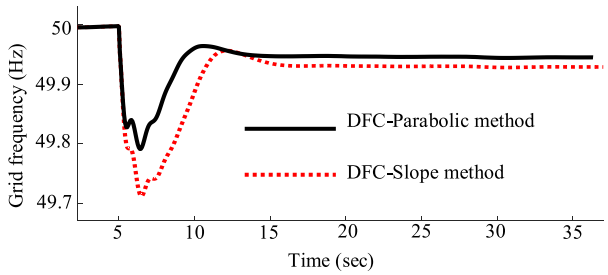

Fig. 18. Variation of frequency.

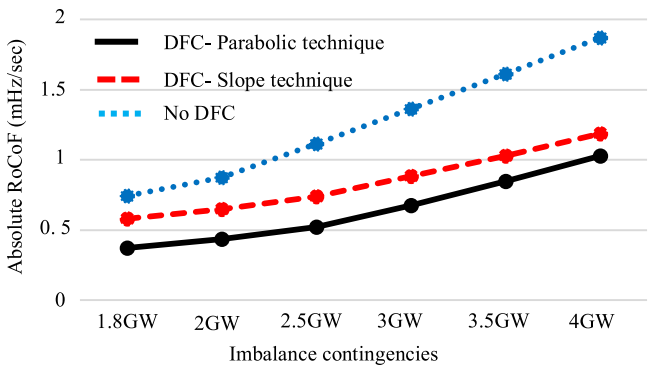

Fig. 19. Maximum values of RoCoF between time 400 ms and 500 ms, following events range from 1.8 GW to 4 GW. Heq = 3 sec.

Fig. 18 shows that a population of heat pumps using the parabolic control technique has reduced the frequency drop more than the slope technique.

Fig. 19 shows the maximum RoCoF between 400 msec to 500 msec, following frequency events ranges from 1.8 GW to 4 GW. Fig. 19 shows that the RoCoF was reduced in each event. This is because the parabolic method had assigned to each heat pump an F_{OFF} closer to $\mathrm{F_{N1}}$ comparing with the linear method. Hence, the DFC caused more heat pumps to respond within the first 500 msec following the frequency event and the frequency deviation was halted earlier.

VIII. Conclusion

A thermodynamic model of a population of domestic heat pumps was developed. A model representing 5,000 heat pumps was identified as an appropriate model and multiple units used to represent the entire population of heat pumps, connected to the GB power system.

A dynamic frequency controller was developed to allow the heat pumps to alter their power consumption in response to system frequency. The trigger frequencies were improved by using a parabolic shape. The frequency control does not interfere with the temperature control of the buildings.

The model of a population of heat pumps was then incorporated into a reduced Great Britain transmission/generation system model. Case studies showed that the power consumption of dynamically controlled heat pumps distributed over GB zones was reduced immediately following a frequency drop. Following a loss of generation, the deviation of grid frequency was reduced with the immediate load change of heat pumps. The power drawn from frequency-sensitive generators was also reduced.

A population of controlled heat pumps can provide an opportunity to restore the system frequency by using stand-by generation (responding after 30 minutes), instead of costly spinning reserve.

Acknowledgment

The authors would like to acknowledge Dr. Y. Li and Dr. R. Lerna, and the employees at National Grid for facilitating the collaboration visit to National Grid and using the transmission GB power system model. The authors would also like to thank Element Energy for sharing the heat pumps data which was used in this study.

References

[1] UK National Grid, "Frequency response, National Grid," 2015. [Online]. Available: http://www2.nationalgrid.com/uk/services/balancing-services/frequency-response/. Accessed on: Oct. 1, 2016.
[2] National Grid plc, "The Grid Code Issue 5 Revision 18," Aug. 2016. [Online]. Available: http://www2.nationalgrid.com/uk/industry-information/electricity-codes/grid-code/the-grid-code/
[3] UK National Grid, "2016 Future energy scenario," Jul. 2016. [Online]. Available: http://fes.nationalgrid.com/
[4] UK National Grid, "Enhanced frequency control capability (EFCC)," Oct. 2014. [Online]. Available: https://www.ofgem.gov.uk/ofgem-publications/87210/ispefccnget.pdf
[5] UK National Grid, "System operability framework 2015," Nov. 2015. [Online]. Available: http://www2.nationalgrid.com/UK/Industry-information/Future-of-Energy/System-Operability-Framework/
[6] The Parliamentary Office of Science and Technology, "Electricity demand-side response," Jan. 2014. [Online]. Available: http://researchbriefings.parliament.uk/ResearchBriefing/Summary/POST-PN-452
[7] National Grid plc, "Frequency control by demand management (FCDM)," Sep. 2017. [Online]. Available: https://www.nationalgrid.com/sites/default/files/documents/FCDM%20v1.1.pdf. Accessed on: May 1, 2016.
[8] S. A. Pourmousavi and M. H. Nehrir, "Real-time central demand response for primary frequency regulation in microgrids," *IEEE Trans. Smart Grid*, vol. 3, no. 4, pp. 1988–1996, Dec. 2012.
[9] N. Lu and Y. Zhang, "Design considerations of a centralized load controller using thermostatically controlled appliances for continuous regulation reserves," *IEEE Trans. Smart Grid*, vol. 4, no. 2, pp. 914–921, Jun. 2013.
[10] J. Kondoh, N. Lu, and D. J. Hammerstrom, "An evaluation of the water heater load potential for providing regulation service," *IEEE Trans. Power Syst.*, vol. 26, no. 3, pp. 1309–1316, Aug. 2011.
[11] N. Lu, "An evaluation of the HVAC load potential for providing load balancing service," *IEEE Trans. Smart Grid*, vol. 3, no. 3, pp. 1263–1270, Sep. 2012.
[12] A. Molina-Garcia, F. Bouffard, and D. S. Kirschen, "Decentralized demand-side contribution to primary frequency control," *IEEE Trans. Power Syst.*, vol. 26, no. 1, pp. 411–419, Feb. 2011.

[13] J. A. Short, D. G. Infield, and L. L. Freris, "Stabilization of grid frequency through dynamic demand control," *IEEE Trans. Power Syst.*, vol. 22, no. 3, pp. 1284–1293, Aug. 2007.
[14] M. Cheng *et al.*, "Power system frequency response from the control of bitumen tanks," *IEEE Trans. Power Syst.*, vol. 31, no. 3, pp. 1769–1778, May 2016.
[15] M. Cheng, S. S. Sami, and J. Wu, "Benefits of using virtual energy storage system for power system frequency response," *Appl. Energy*, vol. 194, pp. 376–385, 2016.
[16] D. G. Infield, J. Short, C. Horne, and L. L. Freris, "Potential for domestic dynamic demand-side management in the UK," in *Proc. IEEE Power Eng. Soc. Gen. Meeting*, 2007, pp. 1–6.
[17] Element Energy, "Frequency sensitive electric vehicle and heat pump power consumption," Jul. 2015.
[18] Z. T. Taylor, K. Gowri, and S. Katipamula, "GridLAB-D technical support document: Residential end-use module version 1.0," Pacific Northwest Nat. Lab., Richland, WA, USA, Jul. 2008.
[19] N. Lu, J. Zhang, P. Du, and Y. V. Makarov, "Controller for thermostatically controlled loads," U. S. Patent 9 362 749, 2013.
[20] J. Hong, N. J. Kelly, I. Richardson, and M. Thomson, "Assessing heat pumps as flexible load," *Proc. Inst. Mech. Eng. A, J. Power Energy*, vol. 227, pp. 30–42, 2013.
[21] V. Dimitriou, "Lumped parameter thermal modelling for UK domestic buildings based on measured operational data," Ph.D. dissertation, Loughborough Univ., Loughborough, U.K., 2016.
[22] G. Strbac, "Demand side management: Benefits and challenges," *Energy Policy*, vol. 36, pp. 4419–4426, 2008.
[23] R. Green, "The effects of cycling on heat pump performance," Dept. Energy Climate Change, London, U.K., Nov. 2012. [Online]. Available: https://www.gov.uk/government/uploads/system/uploads/attachment_data/file/65695/7389-effects-cycling-heat-pump-performance.pdf
[24] DCLG, "Table 401: Household projections," Dept. Communities Local Government, London, U.K., 2016.
[25] NRS, "Table1: Household estimates for Scotland by council area," Nat. Rec. Scotland, Edinburgh, U.K., 2016.
[26] National Grid, "DNO: Distribution Network Operators in the UK," 2016. [Online]. Available: http://www.ovoenergy.com/guides/energy-guides/dno.html. Accessed on: Feb. 1, 2018.
[27] UK National Grid, "Report of the National Grid Investigation into the frequency deviation and automatic demand disconnection that occurred on the 27th May 2008," Feb. 2009. [Online]. Available: http://www.nationalgrid.com/NR/rdonlyres/E19B4740-C056-4795-A567-91725ECF799B/32165/PublicFrequencyDeviationReport.pdf
[28] National Grid, "Frequency changes during large disturbances and their impact on the total system," National Grid, Warwick, U.K., Aug. 2013.
[29] M. T. Muhssin, L. M. Cipcigan, N. Jenkins, M. Cheng, and Z. A. Obaid, "Modelling of a population of Heat Pumps as a Source of load in the Great Britain power system," in *Proc. 2016 Int. Conf. Smart Syst. Tech. (SST)*, 2016, pp. 109–113.

Mazin T. Muhssin (M'15) received the B.Sc. degree in control and systems engineering from the University of Technology, Baghdad, Iraq, in 2006, and the M.Sc. degree in control and automation engineering from University Putra Malaysia, Selangor, Malaysia, in 2010. He is currently working toward the Ph.D. degree in electrical and electronic engineering at Cardiff University, Cardiff, U.K.

He was engaged in the EPSRC project "Ebbs and Flows of Energy Systems." His main research interests include smart grids, flexible demand control, balancing services, and dynamic demand response.

Liana M. Cipcigan (M'08) is a Reader with the School of Engineering, Centre for Integrated Renewable Energy Generation and Supply, Cardiff University, Cardiff, U.K. Her research experience covers power system analysis and control, smart grids, virtual power plants, and DER integration in distribution networks.

She is leading the research of electric vehicles integration and control in distribution networks. She has collaborated widely with industry, more recently during her secondment at National Grid under Royal Academy of Engineering industrial fellowship, working in the Energy Insights Department responsible for the Future Energy Scenarios. She has authored/coauthored around 100 scientific papers, book chapters, and conference papers.

Nick Jenkins (M'81–SM'97–F'05) received the B.Sc. degree from Southampton University, Southampton, U.K., in 1974, the M.Sc. degree from Reading University, Reading, U.K., in 1975, and the Ph.D. degree from Imperial College London, London, U.K., in 1986.

He is currently a Professor and Director of the Institute of Energy, Cardiff University, Cardiff, U.K. Before moving to academia, his career included 14 years of industrial experience, of which 5 years were in developing countries. While working in higher education, he has developed teaching and research activities in both electrical power engineering and renewable energy.

Shane Slater is the Director of Element Energy Ltd, Cambridge, U.K. He brings multi-disciplinary engineering design skills to the practice. His expertise on energy and the built environment had its origins at Max Fordhams Engineers, after which he led the Sustainability and Renewables group at engineering consultants Whitby Bird.

Meng Cheng received the B.Sc. degree in electrical and electronic engineering from Cardiff University, Cardiff, U.K., and North China Electrical Power University, Beijing, China, in 2011, and the Ph.D. degree from Cardiff University in 2015.

She is a Research Associate with Cardiff University. Her main research interests include smart grids and dynamic demand.

Zeyad A. Obaid (M'15) received the B.Sc. degree in control and systems engineering from the University of Technology, Baghdad, Iraq, in 2006, and the M.Sc. degree in control and automation engineering from University Putra Malaysia, Selangor, Malaysia, in 2010. He is currently working toward the Ph.D. degree in electrical and electronic engineering at Cardiff University, Cardiff, U.K.

His main research interests include intelligent control and optimization applications with the power systems.